THE JOURNAL OF BIOLOGICAL CHEMISTRY VOL. 287, NO. 48, pp. 40525–40534, November 23, 2012

The Stem Region of Premembrane Protein Plays an Important Role in the Virus Surface Protein Rearrangement during Dengue Maturation*

Received for publication, May 22, 2012, and in revised form, September 26, 2012 Published, JBC Papers in Press, October 3, 2012, DOI 10.1074/jbc.M112.384446

Qian Zhang[‡§], Cornelia Hunke[¶], Yin Hoe Yau[¶], Vernon Seow[‡§1], Sumarlin Lee[‡§], Lukas Bahati Tanner[‖], Xue Li Guan[**], Markus R. Wenk[‖], Guntur Fibriansah[‡§], Pau Ling Chew[‡§], Petra Kukkaro[‡§], Goran Biuković[¶], Pei-Yong Shi[‡‡], Susana Geifman Shochat[¶], Gerhard Grüber[¶], and Shee-Mei Lok[‡§2]

*From the [‡]Program in Emerging Infectious Diseases, Duke-NUS Graduate Medical School, KTP Building, 8 College Road, Singapore 169857, the [§]Center for Bioimaging Sciences, Department of Biological Sciences, National University of Singapore, Singapore 119077, the [¶]Division of Structural Biology and Biochemistry, School of Biological Sciences, Nanyang Technological, 60 Nanyang Drive, Singapore 637551, [‡‡]Wadsworth Center, New York State Department of Health, Albany, New York 12201, the [‖]Department of Biochemistry, National University of Singapore, 8 Medical Drive, Block MD 7, Singapore 117597, and the **Department of Medical Parasitology and Infection Biology, Swiss Tropical and Public Health Institute, Socinstrasse 57, 4002 Basel, Switzerland*

Background: Dengue virus surface proteins, envelope (E) and pre-membrane (prM), undergo rearrangement during the maturation process at acidic condition.
Results: prM-stem region binds tighter to both E protein and lipid membrane when environment becomes acidic.
Conclusion: At acidic condition, E proteins are attracted to the membrane-associated prM-stem.
Significance: prM-stem region induces virus structural changes during maturation.

Newly assembled dengue viruses (DENV) undergo maturation to become infectious particles. The maturation process involves major rearrangement of virus surface premembrane (prM) and envelope (E) proteins. The prM-E complexes on immature viruses are first assembled as trimeric spikes in the neutral pH environment of the endoplasmic reticulum. When the virus is transported to the low pH environment of the exosomes, these spikes rearrange into dimeric structures, which lie parallel to the virus lipid envelope. The proteins involved in driving this process are unknown. Previous cryoelectron microscopy studies of the mature DENV showed that the prM-stem region (residues 111–131) is membrane-associated and may interact with the E proteins. Here we investigated the prM-stem region in modulating the virus maturation process. The binding of the prM-stem region to the E protein was shown to increase significantly at low pH compared with neutral pH in ELISAs and surface plasmon resonance studies. In addition, the affinity of the prM-stem region for the liposome, as measured by fluorescence correlation spectroscopy, was also increased when pH is lowered. These results suggest that the prM-stem region forms a tight association with the virus membrane and attracts the associated E protein in the low pH environment of exosomes. This will lead to the surface protein rearrangement observed during maturation.

Dengue virus (DENV),[3] a member of the family *Flaviviridae*, is a major human pathogen transmitted by mosquitoes (1). It causes diseases ranging from the mild dengue fever to the severe dengue hemorrhagic fever (2). The 11-kb positive sense RNA genome encodes three structural proteins (capsid, prM, and E) and seven nonstructural proteins (NS1, NS2a, NS2b, NS3, NS4a, NS4b, and NS5) (1). The virus particle consists of an RNA-capsid protein complex, surrounded by a bilayer lipid membrane. The proteins present on the surface of the dengue immature virus are the E and prM (3). The mature virus surface, on the other hand, contains E and M proteins (a cleaved derivative of prM) (4).

The E protein is the major surface antigenic structure on dengue virus. It is involved in receptor binding and fusion. The E protein consists of three domains, namely E-DI, E-DII, and E-DIII (5–7). E-DIII participates in both receptor binding and fusion, whereas E-DII is involved mainly in fusion. E-DII contains a hydrophobic fusion loop at its distal end. During virus infection, the acidic environment of the host cell endosomes will stimulate the exposure of the E-DII fusion loop. This facilitates fusion of the virus membrane to endosomal membrane leading to the release of viral genome into the cell cytoplasm (8, 9).

The prM consists of an N-terminal pr domain followed by the M protein (10) (Fig. 1*A*). The intersection between the pr molecule and M protein contains a furin cleavage site (10). The M protein consists of a linear structure followed by a stem region and two transmembrane helices (11, 12) (Fig. 1*A*). The

* This work was supported by Duke-NUS Graduate Medical School Block Grant R913-200-039-304 and Biomedical Research Council Grant R-913-300-019-304 (to S.-M. L.).
[1] Present address: Institute for Molecular Bioscience, University of Queensland, 306 Carmody Road, QLD 4072, Australia.
[2] To whom correspondence should be addressed. E-mail: sheemei.lok@duke-nus.edu.sg.

[3] The abbreviations used are: DENV, dengue virus; E, envelope; FCS, fluorescence correlation spectroscopy; PC, phosphatidylcholine; PE, phosphatidylethanolamine; PI, phosphatidylinositol; prM, premembrane; PS, phosphatidylserine; RU, response units; SA, streptavidin; SPR, surface plasmon resonance; TFE, 2,2,2-trifluoroethanol; TGN, *trans*-Golgi network.

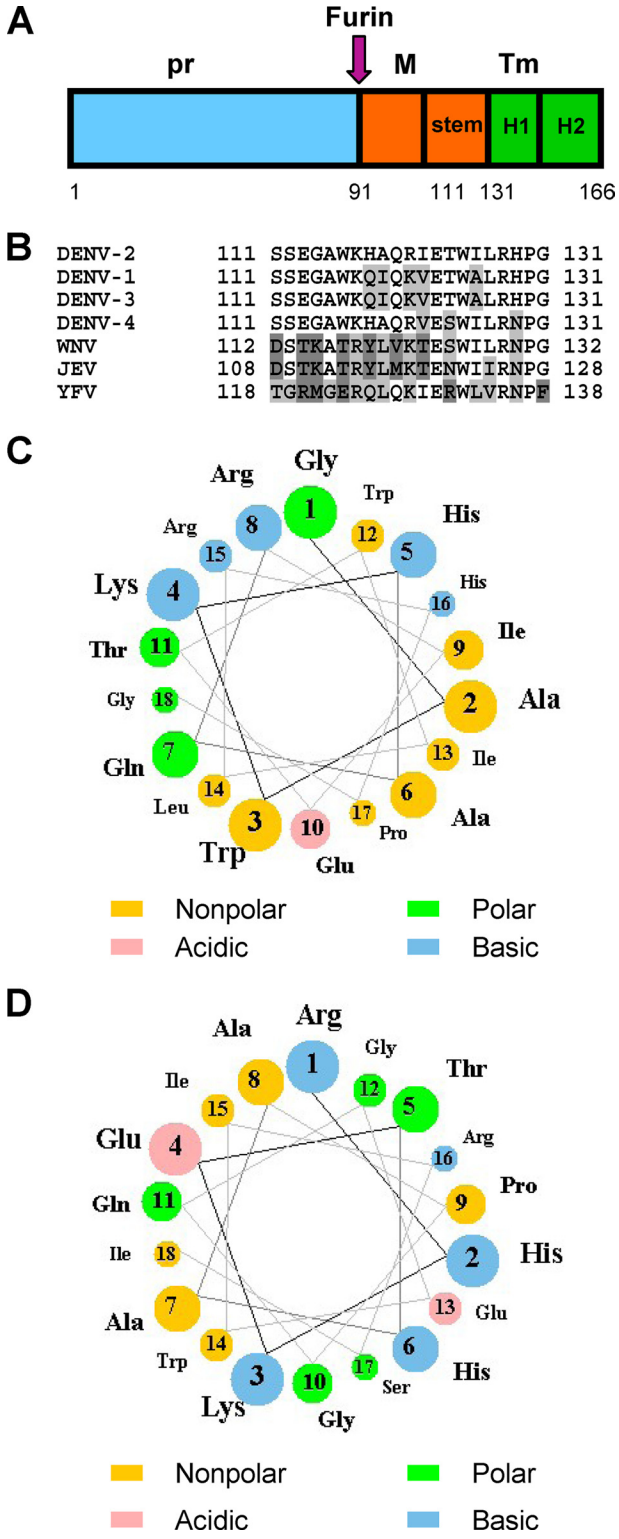

FIGURE 1. **The DENV prM-stem region.** *A*, dengue virus prM molecule consisting of pr (*light blue*), M protein (*orange*), and transmembrane helices (*Tm*) (*green*). During maturation, furin protease (*purple arrow*) cleaves pr, leaving behind the M protein anchored to the surface of mature virus by the transmembrane region. *B*, amino acid sequence alignment of dengue serotype 2 (DENV-2) prM-stem region with other dengue serotypes (DENV-1, DENV-3, and DENV-4), West Nile virus (WNV), Japanese encephalitis virus (JEV), and yellow fever virus (YFV). *Shaded* in *light gray* are residues that have chemical properties similar to those in dengue serotype 2 prM-stem region whereas the residues *shaded* in *dark gray* are different. Conserved residues are not shaded. *C*, helical wheel projection of the prM-stem peptide indicating that the peptide is amphipathic. *D*, helical wheel prediction of the scrambled peptide structure.

stem is mainly an α-helical structure as observed in the cryo-EM map of the mature DENV, and it interacts with the viral lipid membrane (11). The crystal structure of the prM and E complex has been solved previously (10). Only the electron densities of the pr and E proteins were observed, indicating that most of the M protein is flexible. The pr molecule consists mainly of β-strands, and it covers the fusion loop of the E protein, consistent with its function in preventing newly synthesized immature virus from fusing back into the cell in the low pH environment of the *trans*-Golgi network (TGN) and exosomes (12, 13).

Newly synthesized virus particles are first assembled in the endoplasmic reticulum and mature as they pass through the TGN and exosomes (12). During this process, the virus surface proteins undergo major rearrangement in response to the low pH environment of the TGN and exosomes. The structures of the virus before (11) and after maturation (12) have been solved previously by cryo-EM (Fig. 2*A*). When the virus is first synthesized in the neutral pH environment of the endoplasmic reticulum, the prM-E heterodimers are organized as 60 trimeric spikes (Fig. 2, *A* and *B*). In the low pH environment of the TGN and exosomes, the prM-E proteins form dimers that lay parallel to the virus lipid envelope (Fig. 2, *A* and *B*). This structural change exposes the furin cleavage site on prM (12). The cleaved pr molecule, however, remains associated with the fusion loop of the E protein due to the low pH environment and only dissociates from the virus when released outside the cell presumably due to the change in pH (12, 13).

The interactions that trigger the prM-E proteins on the immature virus to rearrange when exposed to low pH are largely unknown. E protein is unlikely to modulate this movement, as the recombinant E ectodomain alone changes from a dimeric to trimeric structure at low pH in the presence of liposomes (8, 9, 14). This is in sharp contrast to the immature virus, where the E protein moves from a trimeric structure to a dimeric one, even though the trimeric structure is different from the postfusion E ectodomain structure. The crystal structures of prM-E at neutral and low pH (10) showed no differences in the interaction of pr molecule with E protein, indicating that the pr molecule is probably not involved in the rearrangement of immature surface proteins. Comparison of the cryo-EM structures of the immature and mature virus showed that in the mature virus, the M proteins have moved closer to the E proteins (Fig. 2*C*) (7). The close proximity (~8 Å in distance) of the residues between the M-stem region and the E protein in the mature virus structure suggests that new interactions have formed during maturation (11) (Fig. 2*D*). This indicates that the M-stem region may play a role in attracting the E protein closer to the viral membrane during maturation. Thus, we investigated the binding properties of the prM-stem region at neutral and low pH conditions. We showed that the prM-stem peptide has increased affinity to the E protein when pH is lowered. The prM-stem peptide also exhibited tighter binding to lipid membrane at low pH compared with neutral pH. The results suggest that in low pH environment, the membrane-associated prM-stem region attracts E proteins closer to the virus membrane thus causing surface protein rearrangement.

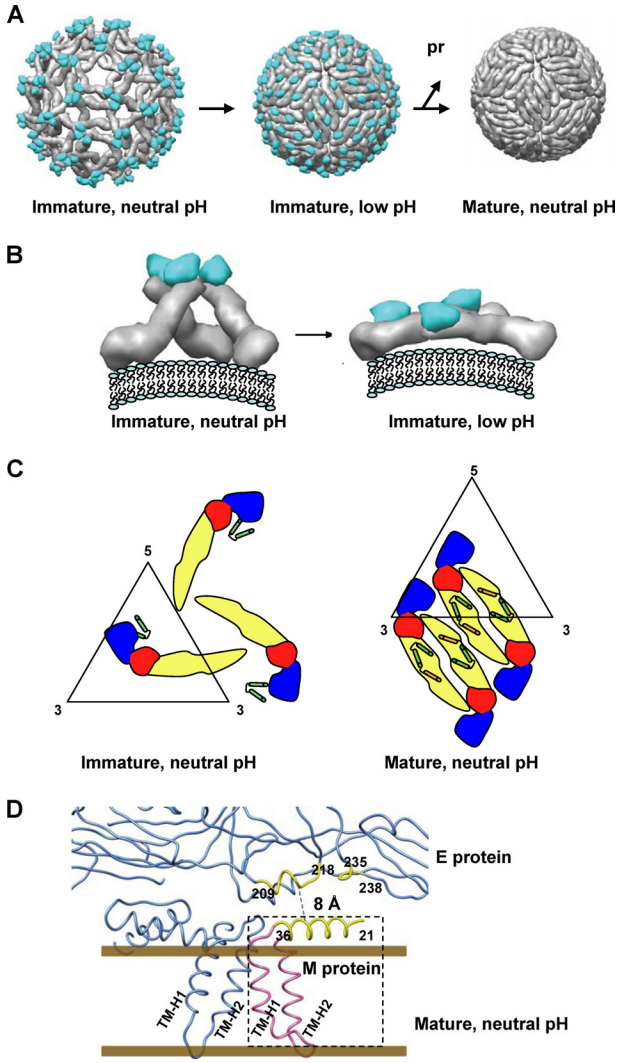

FIGURE 2. **Structural rearrangement of immature virus surface proteins during dengue virus maturation.** *A*, surface representation of fitted prM and E proteins in the cryo-EM maps of immature virus is shown at neutral (7) and low pH (12). When immature virus is assembled in the neutral pH environment of the endoplasmic reticulum, the pr-E protein complex exists as trimeric spikes. In the acidic environment of TGN and exosomes, pr-E complex rearranges to form dimers. E and pr molecules are *colored* in *gray* and *cyan*, respectively. *B*, side view of pr-E trimeric spike on the lipid envelope of the immature virus is shown at neutral pH (*left*) and the dimeric structure after exposure to low pH (*right*) (12). *C*, after dengue virus maturation, the M and E proteins move closer to each other. Positions of the fitted E proteins and prM transmembrane helices in the immature virus (*left*) and the E and M proteins (consisting of M-stem and transmembrane helices) in the mature virus (*right*) are shown in cryo-EM maps at neutral pH (7). Domains I, II, and III of the E protein are *colored* in *red*, *yellow*, and *blue*, respectively. The transmembrane helices of M protein are *colored* in *green* whereas the stem regions are *colored* in *pink*. Due to the medium resolution of the immature virus map, the density of the stem region of the prM is not resolved. *Black triangle* represents an asymmetric unit. *D*, the M-stem region observed in the cryo-EM map of the mature virus (11) is helical in structure, and it interacts with both E protein and the outer leaflet of the bilayer lipid membrane. M protein (in the *dashed rectangle*) and E protein are *colored* in *pink* and *light blue*, respectively. The boundaries of the lipid membrane are indicated as *brown bars*. The potential interacting residues between M (residues 21–36) and E protein (residues 209–218 and 218–235) are *colored* in *yellow*.

EXPERIMENTAL PROCEDURES

Peptides—Peptides containing the prM-stem region sequence (SSEGAWKHAQRIETWILRHPG) (Fig. 1, *B* and *C*) and scrambled sequence (WLSRHKETHAAPGQGEWIRSI) (Fig. 1*D*) were purchased from Peptide Synthesis Core Facility in Nanyang Technological University, Singapore. Peptides were >95% pure, and the amino acid sequence and molecular mass were confirmed by MALDI-TOF mass spectrometry. The unlabeled peptide and biotinylated peptide stocks were prepared in H_2O, and Atto488 dye-labeled peptide was dissolved in H_2O with 20% (v/v) dimethyl sulfoxide (Sigma).

Purification of Dengue Serotype 2 Virus for ELISAs and Lipid Analysis—For ELISAs, immature virus was produced in furin-deficient human adenocarcinoma LoVo cells, (Animal Tissue Culture Collections (ATCC) CCL-229) (15). LoVo cells were infected with mature dengue serotype 2 New Guinea C strain at a multiplicity of infection of 10 for 2 h at 37 °C. At 2 h after infection, the virus was removed, and cells were washed twice with phosphate-buffered saline (PBS). Fresh Ham's F-12 Nutrient Mix (Life Technologies) supplemented with 5% fetal bovine serum (Life Technologies) was then layered on the cells and further incubated at 37 °C, 5% CO_2. At 48–60 h after infection, the tissue culture supernatant containing immature viral particles was harvested, and immature virus was concentrated by centrifugation at 45,000 rpm in a type 70 Ti rotor (Beckman Coulter) for 2 h at 4 °C. The pellet was resuspended in NTE buffer (12 mM Tris at pH 8.0, 120 mM NaCl, and 1 mM EDTA) and stored at −80 °C for future use.

For lipid analysis, mature virus was produced in C6/36 mosquito cells (ATCC CRL-1660). Cells were infected at a multiplicity of infection of 1, and virus was harvested 96 h after infection. Virus particles in supernatant were precipitated by addition of 8% PEG 8000 (w/v, Sigma) and incubating the mixture overnight at 4 °C. The precipitated virus was harvested by centrifugation with JA-10 (Beckman Coulter) at 9000 rpm, for 30 min at 4 °C. The resulting pellet was further purified through 24% (w/v) sucrose cushion (Sigma) by centrifugation at 32,000 rpm for 1.5 h at 4 °C in a type 70 Ti rotor. The pellet was resuspended in NTE buffer and further separated through a linear 10–30% (w/v) potassium tartrate-glycerol gradient (Sigma) by centrifugation at 32,000 rpm for 2 h at 4 °C in a type SW41 rotor (Beckman Coulter). The band containing the virus was collected, buffer-exchanged into NTE buffer, and concentrated using an Amicon Ultra-4 100 kDa MWCO concentrator (Millipore). The purity of immature dengue virus was examined using SDS-polyacrylamide gel.

Purification of Dengue Serotype 2 Soluble E Protein—*Drosophila melanogaster* Schneider 2 cells (Life Technologies) were transfected with recombinant pMT/BiP/V5-HisA plasmid encoding dengue virus serotype-2 E protein ectodomain (residues 1–394). The expressed soluble E protein was initially purified by passing the tissue culture supernatant through a column filled with the 4G2 antibody (ATCC HB-112) cross-linked resin. The E protein was then further purified by size exclusion chromatography using a Superdex 200 10/300 GL column (GE Healthcare) in 20 mM potassium phosphate, pH 7.0, with 120 mM NaCl.

Virus Lipid Analysis—Total lipids were extracted as described previously (16) using a modified version of the Bligh and Dyer extraction method (17). All buffers were prechilled, and the extraction was performed on ice. Briefly, C6/36 cells or purified dengue virus serotype 2 was resuspended in 50 μl of

PBS and incubated with 200 μl of chloroform and 400 μl of methanol. The mixture was vortexed three times for a duration of 1 min each, with a 4-min incubation on ice between each vortexing. Then, 300 μl of chloroform and 200 μl of 1 M KCl were added to each tube and vortexed three times each for 30 s with 1-min intervals. The aqueous phase and organic phase were separated by centrifugation at 9000 rpm for 2 min, and the lower organic phase was transferred to a fresh tube. Samples were dried using a speed vacuum.

Individual classes of phosphatidylserine (PS), phosphatidylethanolamine (PE), phosphatidylinositol (PI), and phosphatidylcholine (PC) were analyzed by multiple reaction monitoring using chromatographic separation techniques. Only HPLC grade solvents were used, and lipid standards were obtained from Avanti Polar Lipids. Briefly, cell lipid extracts were dissolved in chloroform:methanol mixture (ratio of 1:1), then separated with an Agilent 1200 HPLC system before analyzing with a 3200 Q-Trap mass spectrometer (Life Technologies). Signal intensities for each lipid species were normalized to corresponding internal standards: dimyristoylglycero-3-phosphoserine (C14PS), 1,2-diheptadecanoylglycero-3-phosphoethanolamine (C17PE), 1,2-dioctanoylglycero-3-phosphoinositol (C8PI), 1,2-dinonadecanoylglycero-3-phosphocholine (C19PC), and represented as molar fractions of the total amount of measured phospholipids.

Circular Dichroism Spectroscopy—The peptide stock was diluted to 200 μM in 20 mM potassium phosphate, pH 6.0, or pH 8.0 with increasing concentrations of 2,2,2-trifluoroethanol (TFE) (0, 10%, 20%, 30%, 40%, 50% V/V). The CD spectra were recorded on a CHIRASCAN spectropolarimeter (Applied Photophysics) using a quartz cell with 0.01 cm pathlength (Hellma). Each spectrum is an average of three consecutive scans from wavelength of 180–260 nm using a bandwidth of 1 nm and a response time of 2 s. Spectra of control buffer with corresponding concentration of TFE were subtracted from the peptide spectra. The CD signals were converted into molar ellipticity in units of degree*·cm^{2*}·dmol^{-1} using the equation $[\theta] = \theta/(10 \times C \times N_p \times l)$. Where θ is the ellipticity in millidegrees, C is the peptide molar concentration (M), and l is the cell pathlength (cm). The percentage of helical content of the peptide was analyzed using K2D3 software (18).

Liposome Preparation—Liposomes were composed of 6:3:1 molar ratio of 1,2-dioleoyl-*sn*-glycero-3-phosphocholine (DOPC), 1,2-dioleoyl-*sn*-glycero-3-phosphoethanolamine (DOPE), and 1,2-dioleoyl-*sn*-glycero-3-phospho-L-serine (DOPS) (Avanti Polar Lipids). The components dissolved in chloroform were mixed and dried under vacuum for at least 2 h. The lipid film was rehydrated in 20 mM potassium phosphate, pH 6.0 or pH 8.0, 120 mM NaCl for >60 min at 30 °C with shaking. The suspension was subjected to five freeze-thaw cycles, followed by 30 cycles of extrusion through a 0.1-μm Whatman polycarbonate filter (GE Healthcare). The quality of the liposomes was determined by Zetasizer Nano S dynamic light scattering (Malvern Instruments).

Fluorescence Correlation Spectroscopy—Fluorescence correlation spectroscopy (FCS) was performed on a LSM 510 Meta/ConfoCor 3 (Zeiss, Germany) using Atto488-prM-stem peptide. For the FCS experiment, 20 mM potassium phosphate, pH 6.0, and 20 mM potassium phosphate, pH 8.0, buffers were used. The temperature was adjusted to 25 °C in an incubation chamber (Zeiss). The 488-nm 30-mW argon laser was focused into the aqueous solution by a water immersion objective (40 ×/1.2 W Korr UL-VIS-IR, Zeiss). FCS was measured in 15 μl droplets of the diluted Atto488-prM-stem peptide, which were placed on Nunc 8-well chambered cover glass. To prevent nonspecific binding, the cover glasses were treated with 3% solution of gelatin in H_2O, and unbound gelatin was removed by multiple washing steps with H_2O (19). The following filter sets were used: MBS, HFT 488; EF, none; DBS, Mirror; EF2, LP 505. Out-of-focus fluorescence was rejected by a 90 μm pinhole in the detection pathway, resulting in a confocal detection volume of approximately 0.38 fluid ounces. Solution of Atto488 dye in H_2O was used as reference for calibrating the confocal microscope. Variable concentrations of liposome solutions were mixed with Atto488-labeled prM-stem peptide. The drop was incubated on the glass slip surface for 3 min and monitored by FCS. The fluorescence autocorrelation functions were determined by measurements of at least 10 repetitions with 30 s each. To analyze the autocorrelation functions of Atto488-prM-stem peptide bound to the liposomes, models with the diffusion time and the triplet state were used for fitting (FCS-LSM software; ConfoCor 3, Zeiss). The diffusion time of fluorescent peptide was measured independently, and the determined value was kept fixed during the fitting of the FCS data. Based on this, the determination of the binding constants required only the calculation of the relative amounts of free prM-stem peptide with the short diffusion time compared with the increased diffusion time of the prM-stem peptide bound to the larger liposome. Calculations of the bound fractions and the dissociation constants were done by using the ConfoCor 3 software 4.2, Excel 2007, and OriginPro 8 SR4.

ELISA—Microtiter plates (Nunc Maxisorp, Thermo Scientific) were coated with E ectodomain (0.2 μg/well) or immature virus. The plates were then blocked with 3% bovine serum albumin (BSA, w/v; Sigma) at 37 °C for 1 h. Five-fold serial dilutions of biotinylated prM-stem peptide in 20 mM potassium phosphate with 120 mM NaCl, pH 6.0 or pH 8.0, with 2% BSA (w/v) were then added to respective wells and incubated at room temperature for 1 h. For the immature virus, the virus was preincubated with prM-stem peptide for 15 min at pH 8.0 prior to exposure to low pH. The wells were washed five times with respective buffers. Streptavidin (SA) conjugated with Alexa Fluor 488 (Life Technologies) was added to wells and incubated at room temperature for 1 h. The amount of biotinylated peptide interacting with E proteins was determined by detecting for SA-Alexa Fluor 488 at excitation wavelength of 488 nm and emission of 519 nm using an Infinite® 200 microplate reader (Tecan). All ELISA experiments were repeated three times in triplicates, scrambled peptide controls were also included.

Surface Plasmon Resonance (SPR)—Affinities of the prM-stem peptide to E ectodomain at pH 6.0 and pH 8.0 were determined by using Biacore 3000 instrument (GE Healthcare). Approximately 100, 500, and 1500 response units (RU) of biotinylated peptide (prM-stem region peptide or scrambled peptide) were immobilized on a SA sensor chip. Negative control channels were set up where no peptide was immobilized. E ectodomain was dialyzed into 20 mM potassium phosphate, pH

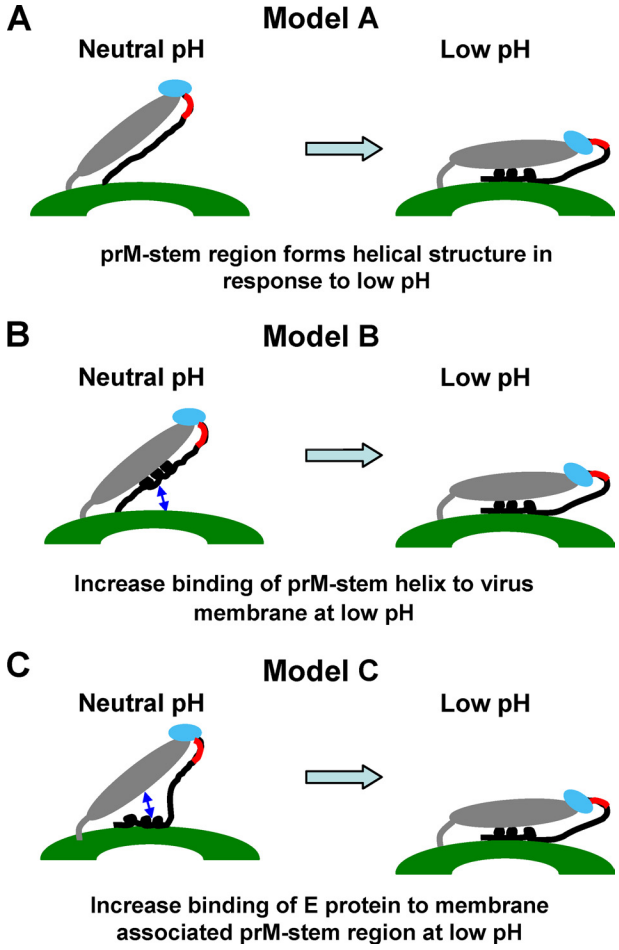

FIGURE 3. **Three proposed ways the prM-stem region could move the E protein closer to the viral membrane at low pH during the DENV maturation process.** *A*, the prM-stem is linear in structure at neutral pH but forms helical structure upon exposure to low pH environment. *B*, the prM-stem region is helical in structure in both pH values but only interacts with the viral lipid surface when pH is lowered. *C*, the membrane-associated prM-stem helix only interacts with the E protein at low pH. The pr molecules are *colored* in *light blue*, M part of the prM is *colored* in *black* and furin cleavage site in *red*. E protein and the bilayer lipid membrane are *colored* in *gray* and *green*, respectively.

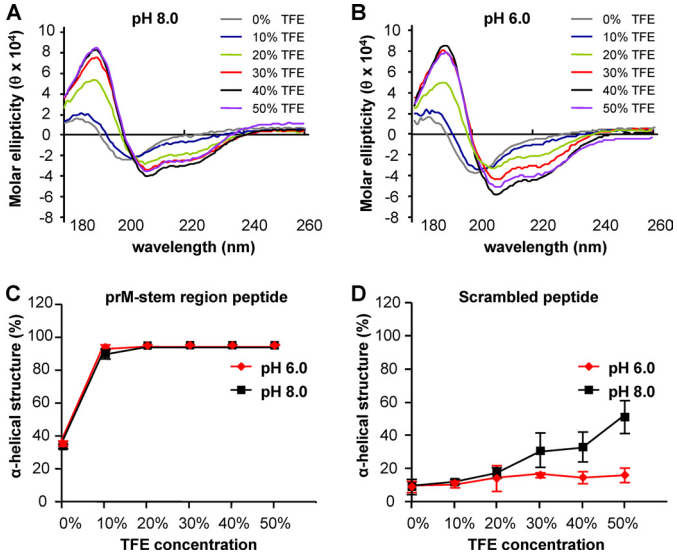

FIGURE 4. **PrM-stem region peptide forms helical structure.** *A* and *B*, CD spectra of the prM-stem peptide is shown in the presence of increasing concentrations of TFE at pH 8.0 (*A*) and pH 6.0 (*B*). *C*, the minimum concentration of TFE required to induce formation of helicity of the peptide at pH 6.0 was similar to that at pH 8.0. The percentage of helicity of prM-stem peptide is plotted against increasing concentrations of TFE. *D*, scrambled peptide showed low levels of helical structure. At pH 6.0, the scrambled peptide did not form helical structure at any tested TFE concentrations. At pH 8.0, the scrambled peptide is ~50% helical when incubated at maximum TFE concentration tested.

6.0 or pH 8.0, buffers with 120 mM NaCl and then concentrated to 2 mg/ml. Sixty μl of 2-fold serial dilutions of the E protein (1:10, 1:20, 1:40, 1:80, 1:160, and 1:320 dilution) were passed through the negative control and test flow cells at a flow rate of 30 μl/min. All experiments were performed in duplicates. The chip was then washed with buffer for 5 min. Regeneration of the surface between injections was done with a 30-s pulse of 50 mM NaOH. The sensorgrams were double-referenced (responses were corrected with both blank buffer injections and the response from the reference flow cell). The binding affinity of E protein to immobilized prM-stem peptide was determined by fitting to a nonlinear 1:1 (Langmuir) binding model, in the BIAevaluation 3.1 software.

RESULTS

We proposed and tested three possible models of how the prM-stem region could pull the E protein closer to the virus lipid membrane in response to low pH (Fig. 3). The first model (model A) requires a structural change of the prM-stem region of immature virus (Fig. 3*A*). The prM-stem region would change its structure from a linear conformation to a helix upon exposure to low pH environment. The second model (model B) implies that the prM-stem region has increased affinity to the lipid envelope at low pH thereby pulling the prM-E complex to the virus lipid surface (Fig. 3*B*). The third model (model C) is based on assumption that the E protein has increased affinity to the membrane-associated prM-stem region at low pH (Fig. 3*C*).

Dengue (Serotype 2) prM-stem Peptide Has a High Propensity to Form Helical Structure at Both Neutral and Low pH—The 9 Å cryo-EM structure of the mature virus showed that the M-stem region exists as a helix (11). However, the densities corresponding to the same prM-stem region were not resolved in the medium resolution maps of the dengue serotype 2 immature virus both at neutral (7) and low pH (12) (12.5 and 25 Å resolution, respectively). Therefore, to detect the structure of the prM-stem region, circular dichroism (CD) spectroscopy was applied using a synthesized peptide consisting of prM residues 111–131 (Fig. 1, *B* and *C*). TFE, a chemical routinely used to promote formation of secondary structures, was included to compare the helical forming properties of the prM-stem peptide at different pH values (20). The rationale behind this experiment is that peptides with a higher tendency to form a helical structure will require a lower TFE concentration to induce the same level of helicity. The CD spectra showed that the prM-stem peptide has a tendency to form a helical structure in the presence of TFE as observed by a typical double absorption minimum at 208 and 222 nm (Fig. 4, *A* and *B*). Analysis by the program K2D3 (18) showed that 10% TFE can induce >90% helical structure of prM-stem peptide at both pH values. In addition, there was no significant difference between pH 6.0 and pH 8.0 in the concentrations of TFE required to induce

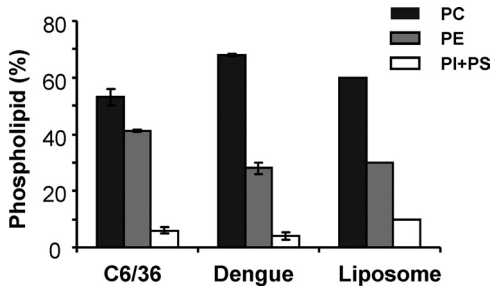

FIGURE 5. **Lipid compositions of DENV, C6/36, and liposome membranes.** The major lipid compositions are expressed as percentages of the total phospholipid.

the maximum percentage of helical structure of the prM-stem peptide (Fig. 4*C*). In contrast, the control scrambled peptide had a much lower helical content at both pH values even at high TFE concentrations (Fig. 4*D*). In conclusion, the prM-stem region of the immature virus is likely to remain helical in structure throughout the dengue virus maturation process.

FCS Analysis Shows That the prM-stem Peptide Has a Higher Binding Affinity to Liposomes at pH 6.0 Compared with pH 8.0—To make liposomes that mimic the virus membrane, lipids were extracted from dengue virus propagated in C6/36 cells and analyzed by Q-Trap mass spectrometry. The analysis showed that the majority of the phospholipids were zwitterionic (PE, PC), and about 6–8% were anionic (PI, PS) (Fig. 5). This is similar to the composition of the endoplasmic reticulum in mammalian cell line as reported previously (21, 22). Therefore, liposomes were made to contain PC:PE:PS in the ratio of 6:3:1.

The ability of prM-stem peptide to bind to liposomes was studied by FCS using Atto488 labeled prM-stem peptide. As a reference, the mean count rate per Atto488 fluorophore was determined to be 55.5 ± 0.4 kHz. Compared with free Atto488 dye, the count rate value of Atto488-prM-stem peptide was 69.2 ± 3.9 kHz at pH 8.0 and 64.1 ± 3.9 at pH 6.0. Fitting the autocorrelation functions resulted in characteristic times of diffusion $\tau_D = 46.2 \pm 1.1$ μs for Atto488 and $\tau_D = 19.0 \pm 1.1$ μs for Atto488-prM-stem peptide at pH 8.0 ($\tau_D = 29.7 \pm 3.3$ μs for Atto488-prM-stem peptide at pH 6.0). Fig. 6*A* shows the fitted autocorrelation curves of Atto488-prM-stem peptide when incubated with a series of concentrations of liposomes at pH 8.0 and 6.0, respectively. The addition of liposomes resulted in a significant change of the mean diffusion time τ_D. The diffusion time for Atto488-prM-stem peptide bound to liposomes was fixed after its determination. The increase of the diffusion time was due to a rise in the mass of the diffusing particle, when Atto488-prM-stem peptide bound to the liposomes. The determined fractions of peptide-liposome assembly *versus* increasing concentrations of liposomes at pH 8.0 and 6.0 are shown in Fig. 6*B*. Affinities (K_D) of liposomes bound to Atto488-prM-stem peptide were 52.1 ± 2.5 μM at pH 8.0 and 6.2 ± 0.3 μM at pH 6.0 (Fig. 6*B*). A concentration-dependent binding was also observed when the Atto488-scrambled peptide was incubated with liposomes at pH 8.0 and pH 6.0 (Fig. 6*C*). However, K_D of liposomes bound to scrambled peptide at pH 8.0 (52.3 ± 2 μM) were not significantly different from that at pH 6.0 (52.2 ± 2.4 μM) (Fig. 6*D*). This affinity is similar to when the prM-stem was incubated with liposome at pH 8.0. In conclusion, the Atto488-prM-stem peptide binds liposome more tightly at pH 6.0 than at pH 8.0, and the increased affinity at low pH is prM-stem sequence-specific.

DENV prM-stem Peptide Interacts with the Ectodomain of E Protein and Virus in a pH-dependent Manner—ELISA was used to examine the binding of prM-stem peptide to the E ectodomain at different pH values. E protein was coated, and the binding of biotinylated prM-stem peptide to the E protein was detected by SA-Alexa Fluor 488. PrM-stem peptide at all concentrations was shown to have higher binding to E protein at pH 6.0 compared with pH 8.0 (Fig. 7*A*). The significance of the difference was examined using one-tailed Student's *t*-test with p value < 0.05. When pH was reversed from low pH to neutral pH, the amount of biotinylated prM-stem peptide binding to E protein was similar to the condition where pH was kept constantly at pH 8.0 (Fig. 7*B*). This is consistent with the observation by cryo-EM that the surface protein rearrangement on immature dengue virus from neutral pH to low pH is reversible (12).

The binding of prM-stem peptide to the immature virus at different pH values was also analyzed by ELISA. At all concentrations, the prM-stem peptide was shown to bind tighter (by ~2-fold) to the immature virus at pH 6.0 compared with pH 8.0 (Fig. 7*C*). The added exogenous prM-stem peptide was able to compete with the virus prM stem region for the E proteins at low pH.

Biotinylated scrambled peptide controls were included in both ELISAs (Fig. 7*A*) with E protein and immature virus, and binding of the control peptide to both antigens was negligible (Fig. 7*C*). These results suggested that binding of the prM-stem peptide to E protein and immature virus is specific.

SPR was used to further study the affinity of the prM-stem to E protein at different pH values. Different amounts of biotinylated prM-stem peptide were captured on SA sensor chip for optimization of the kinetic assay, and a range of concentrations of ectodomain E protein were passed over the chip. When 100 RU of biotinylated prM-stem peptide were captured on the SA surface, <5 RU of E protein were observed to bind to the peptide. Thus, the immobilized biotinylated prM-stem peptide was increased to 500 and 1500 RU. The results showed that approximately three times more E protein bound to prM-stem peptide at pH 6.0 compared with pH 8.0 at all concentrations of E proteins (Fig. 8*A*). When 500 RU of prM-stem peptide was captured, the binding affinity (K_D) of the prM-stem-E complex was 0.29 μM at pH 6.0 and 0.73 μM at pH 8.0 with p value < 0.05; and when 1500 RU was captured, the K_D was 0.34 μM at pH 6.0 and 0.69 μM at pH 8.0. Biotinylated scrambled peptide was also immobilized on the SA chip as a negative control. At both pH 8.0 and pH 6.0, E protein bound weakly to the scrambled peptide (Fig. 8*B*).

DISCUSSION

To study the mechanism of surface protein rearrangement, we have proposed three models (Fig. 3). The results are consistent with models B and C. The prM-stem peptide binds stronger to both liposome (model B) and E protein (model C) at low pH, suggesting that the prM-stem region on the virus could pull the

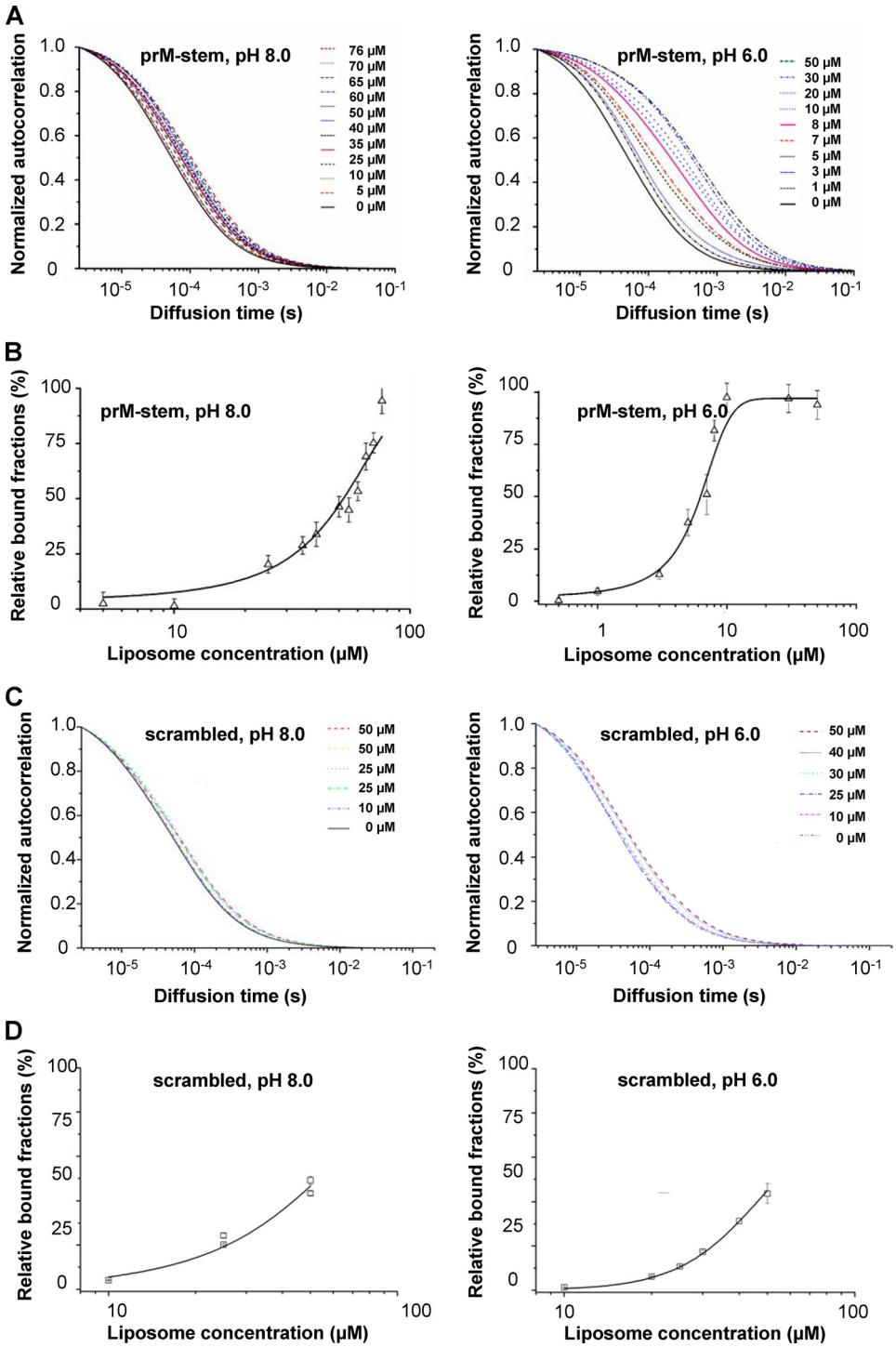

FIGURE 6. **The binding of Atto488-prM-stem peptide and Atto488-scrambled peptide to liposomes.** *A*, concentration-dependent binding traits of Atto488-prM-stem peptide to liposomes. Normalized autocorrelation functions of Atto488-prM-stem peptide in increasing concentrations of liposomes at pH 8.0 and pH 6.0 are shown. *B*, best fits yielding the binding constants represented as a *fitted line* by a nonlinear Boltzmann curve fit at pH 8.0 and pH 6.0. *C*, concentration-dependent binding of Atto488-scrambled peptide to liposomes. *D*, binding constants of the Atto488-srambled peptide to liposomes shown in nonlinear Boltzmann curve fit at pH 8.0 and pH 6.0.

E protein closer to its lipid membrane during maturation. This is consistent with the cryo-EM structures of the immature virus (7, 12) and mature virus (11) at neutral pH (Fig. 2, *C* and *D*). The M protein moves to interact closely with the E protein after the virus has matured.

The increase in binding of the E protein to M-stem region as observed in our study, however, cannot explain the "flip-up" motion of E proteins on mature virus during fusion in the low pH environment of the endosome (8, 9). In contrast to immature virus, the mature virus does not contain pr molecules; and the fusion peptide of the E protein is therefore free to interact with the endosomal membrane. We postulate that the affinity between the E protein fusion loop and the endosomal membrane at low pH may be higher than the interaction between E

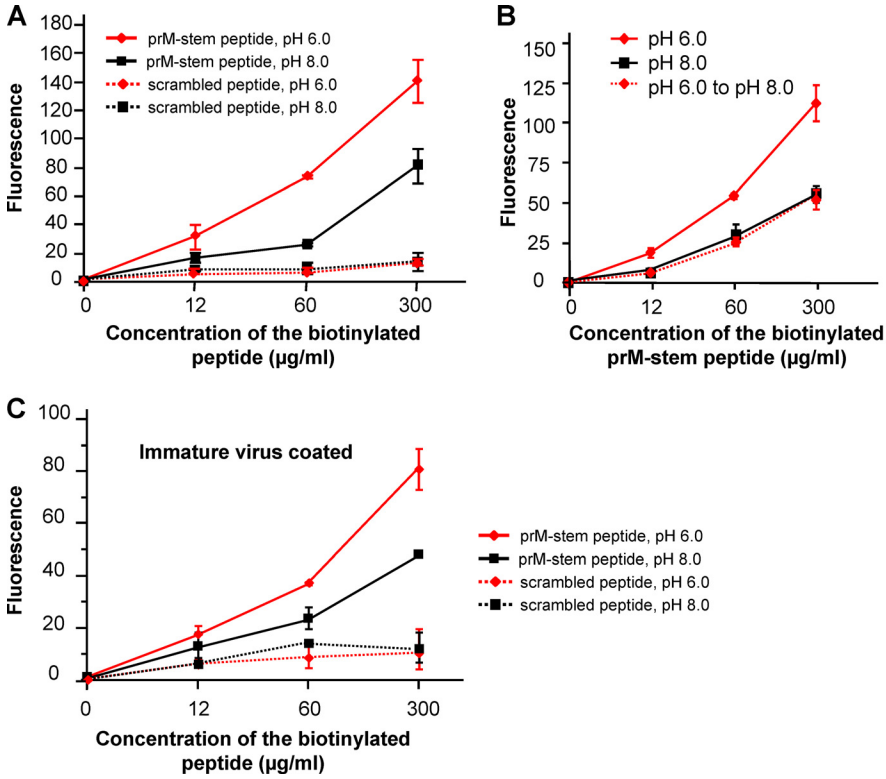

FIGURE 7. **ELISA analysis of the binding of prM-stem peptide to E protein ectodomain and immature virus.** *A*, biotinylated prM-stem peptide binds tighter to the E protein at low pH compared with neutral pH in ELISAs. Fluorescently labeled streptavidin is used to detect the amount of biotinylated prM-stem peptide bound. *B*, binding of prM-stem peptide to E protein is reversible as demonstrated when pH is changed from 6.0 to 8.0. *C*, biotinylated prM-stem peptide binds tighter to the immature virus at low pH compared with neutral pH.

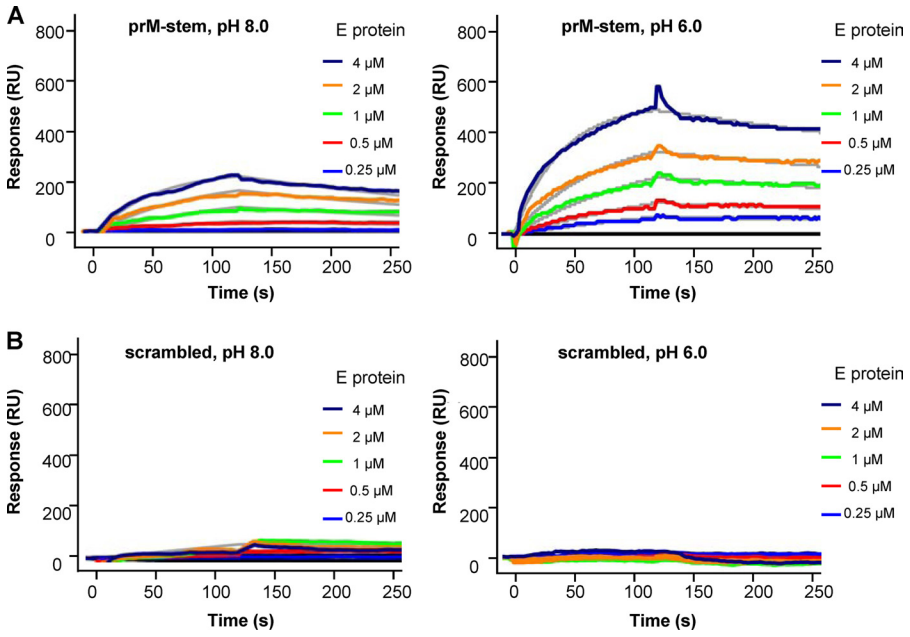

FIGURE 8. **SPR analysis of the binding of prM-stem peptide to E protein ectodomain.** *A*, significant increase in the binding of E protein to captured prM-stem peptide (500 RU) on SA chip was detected at pH 6.0 compared with pH 8.0. The fitted model for each E protein concentration is shown as a *gray line*. *B*, low binding of E protein to captured biotinylated scrambled peptide at both pH 6.0 and pH 8.0 was detected.

and M-stem region, thus allowing E proteins to flip up during fusion. This suggests that the affinity between E with M (or prM)-stem region could be relatively weak. This is consistent with our observation that at low pH, the K_D of E-prM-stem peptide interaction is approximately 0.3 μM. In addition, *in vitro* cultivation of mature dengue virus in mosquito cell lines very often produced a mixture of mature and immature virus (15). This suggests that the maturation process is not efficient, which may be a result of the weak affinity between the E-prM-stem region.

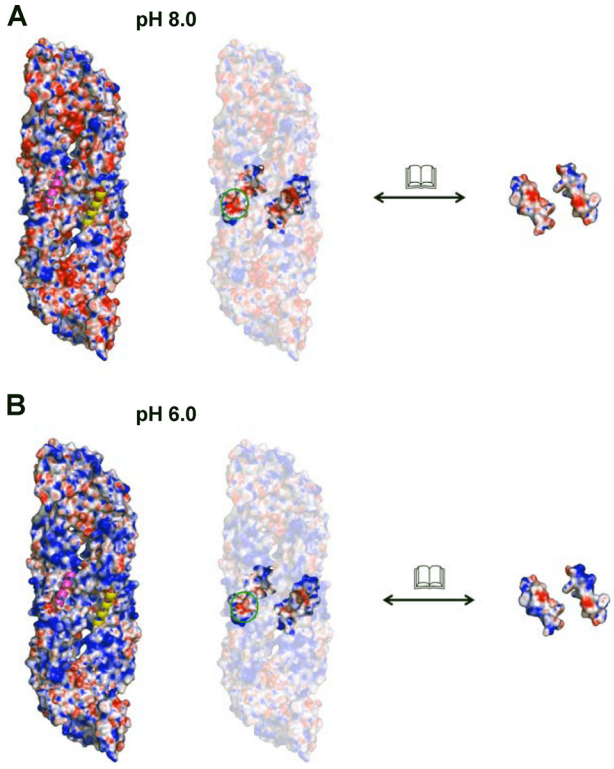

FIGURE 9. **Surface charge changes of the possible interacting interface between the E and the M-stem region in the mature virus at pH 8.0 (*A*) and pH 6.0 (*B*).** *Left panels* show the surface charges of the E protein dimer (highly negatively charged residues in *red* and positively charged residues in *blue*) and also the ribbon structure of the M protein dimers (colored in *yellow* and *pink*). The *center* and *right panels* show the open book representation of the surface electrostatic charges of the interacting interface between E protein dimer and the two M-stem region. The surface negative charges (*circled* in *green*) in the E protein are reduced when pH is lowered to 6.0. This may lower the repulsive force between the E protein and M-stem region leading to an increased in interaction.

Due to the low resolution cryo-EM map (25 Å) of the immature virus at low pH, observations of the interacting interface between prM-stem and E are not possible. However, the likely interacting interface between the M-stem and the E protein indicated in the 9 Å cryo-EM mature virus structure, is based on the assumption that this interaction is similar to that in the immature virus at low pH during maturation. We can analyze the differences in the surface electrostatic charges of the M-stem and E protein interacting interface at pH 8.0 and 6.0 (Fig. 9) by using the programs PDB2PQR and PROPKA (23, 24). This suggests that at pH 6.0, the negatively charged surface on the E protein-interacting interface is reduced, and this may lower the repelling force between the M-stem and the E protein thus allowing binding. The question is, why is this interaction still detected in the mature virus structure at neutral pH? One possibility is that other interactions, *e.g.* between E-E proteins, have been formed, and they stabilize the surface virus structure thus still holding the M-stem to E protein at close proximity to each other.

Other residues may also be important in increasing interaction between the E and prM-stem region. Histidine residues have been shown to act as pH sensors in nature (25, 26). The imidazole side chain of histidine has a p*K* of 6. At pH 7.0 the nonprotonated form is dominant, whereas at pH 6.0 it is double protonated and positively charged. When histidine is positively charged, it may interact with acidic amino acid residues. Based on the fitting of the M-stem region and the E protein in the 9 Å resolution mature virus map (11), there are 2 histidine residues on the M-stem region (residues 28 and 39, equivalent to residues 118 to 129 in prM) and two histidines (residues 209 and 261) on the E protein that might be involved in the prM-stem and E interaction. Comparison of the amino acid sequence of the prM-stem region of flaviviruses (dengue 1, 2, 3, 4, West Nile, kunjin and yellow fever) (Fig. 1*C*) shows that His-118 is only conserved between dengue 2 and 4; His-129 is conserved across dengue serotypes 1, 2, and 3. Both of these histidine residues of dengue 2 virus are absent in yellow fever and West Nile viruses. Comparison of His-209 and His-261 in the E protein with other flaviviruses showed that His-209 is highly conserved among flaviviruses (present in dengue, tick-borne encephalitis, and West Nile viruses, but not in yellow fever virus) whereas His-261 is conserved across dengue serotypes and West Nile virus.

In conclusion, the results suggest that the prM-stem region modulates the immature virus surface protein movement during the dengue virus maturation process. Specifically, an increase in the binding to both the virus lipid membrane and E proteins at low pH was observed, which can bring the E proteins closer to the viral membrane as observed in the cryo-EM map of the immature virus at low pH (12). Compounds designed to inhibit the interaction between E and prM-stem region could potentially be used to reduce the number of infectious mature virus particle.

Acknowledgments—Drosophila S2 cells expressing the soluble E protein were provided by Dr. Long Li and Prof. Michael G. Rossmann, Purdue University, West Lafayette, IN.

REFERENCES

1. Lindenbach, B. D., Thiel, H. J., and Rice, C. M. (2007) in *Fields Virology* (Knipe, D. M., Howley, P. M., Griffin, D. E., Lamb, R. A., Martin, M. A., Roizman, B., and Straus, S. E. eds), 5th Ed., pp. 1101–1152, Lippincott Williams & Wilkins, Baltimore
2. World Health Organization (1997) *Dengue Haemorrhagic Fever: Diagnosis, Treatment, Prevention and Control,* 2nd Ed., pp. 12–23, World Health Organization, Geneva, Switzerland
3. Zhang, Y., Corver, J., Chipman, P. R., Zhang, W., Pletnev, S. V., Sedlak, D., Baker, T. S., Strauss, J. H., Kuhn, R. J., and Rossmann, M. G. (2003) Structures of immature flavivirus particles. *EMBO J.* **22,** 2604–2613
4. Kuhn, R. J., Zhang, W., Rossmann, M. G., Pletnev, S. V., Corver, J., Lenches, E., Jones, C. T., Mukhopadhyay, S., Chipman, P. R., Strauss, E. G., Baker, T. S., and Strauss, J. H. (2002) Structure of dengue virus: implications for flavivirus organization, maturation, and fusion. *Cell* **108,** 717–725
5. Rey, F. A., Heinz, F. X., Mandl, C., Kunz, C., and Harrison, S. C. (1995) The envelope glycoprotein from tick-borne encephalitis virus at 2 Å resolution. *Nature* **375,** 291–298
6. Modis, Y., Ogata, S., Clements, D., and Harrison, S. C. (2003) A ligand-binding pocket in the dengue virus envelope glycoprotein. *Proc. Natl. Acad. Sci. U.S.A.* **100,** 6986–6991
7. Zhang, Y., Zhang, W., Ogata, S., Clements, D., Strauss, J. H., Baker, T. S., Kuhn, R. J., and Rossmann, M. G. (2004) Conformational changes of the flavivirus E glycoprotein. *Structure* **12,** 1607–1618
8. Bressanelli, S., Stiasny, K., Allison, S. L., Stura, E. A., Duquerroy, S., Lescar, J., Heinz, F. X., and Rey, F. A. (2004) Structure of a flavivirus envelope glycoprotein in its low-pH-induced membrane fusion conformation.

EMBO J. **23,** 728–738
9. Modis, Y., Ogata, S., Clements, D., and Harrison, S. C. (2004) Structure of the dengue virus envelope protein after membrane fusion. *Nature* **427,** 313–319
10. Li, L., Lok, S. M., Yu, I. M., Zhang, Y., Kuhn, R. J., Chen, J., and Rossmann, M. G. (2008) The flavivirus precursor membrane-envelope protein complex: structure and maturation. *Science* **319,** 1830–1834
11. Zhang, W., Chipman, P. R., Corver, J., Johnson, P. R., Zhang, Y., Mukhopadhyay, S., Baker, T. S., Strauss, J. H., Rossmann, M. G., and Kuhn, R. J. (2003) Visualization of membrane protein domains by cryo-electron microscopy of dengue virus. *Nat. Struct. Biol.* **10,** 907–912
12. Yu, I. M., Zhang, W., Holdaway, H. A., Li, L., Kostyuchenko, V. A., Chipman, P. R., Kuhn, R. J., Rossmann, M. G., and Chen, J. (2008) Structure of the immature dengue virus at low pH primes proteolytic maturation. *Science* **319,** 1834–1837
13. Yu, I. M., Holdaway, H. A., Chipman, P. R., Kuhn, R. J., Rossmann, M. G., and Chen, J. (2009) Association of the pr peptides with dengue virus at acidic pH blocks membrane fusion. *J. Virol.* **83,** 12101–12107
14. Allison, S. L., Schalich, J., Stiasny, K., Mandl, C. W., Kunz, C., and Heinz, F. X. (1995) Oligomeric rearrangement of tick-borne encephalitis virus envelope proteins induced by an acidic pH. *J. Virol.* **69,** 695–700
15. Zybert, I. A., van der Ende-Metselaar, H., Wilschut, J., and Smit, J. M. (2008) Functional importance of dengue virus maturation: infectious properties of immature virions. *J. Gen. Virol.* **89,** 3047–3051
16. Chan, R., Uchil, P. D., Jin, J., Shui, G., Ott, D. E., Mothes, W., and Wenk, M. R. (2008) Retroviruses human immunodeficiency virus and murine leukemia virus are enriched in phosphoinositides. *J. Virol.* **82,** 11228–11238
17. Bligh, E. G., and Dyer, W. J. (1959) A rapid method of total lipid extraction and purification. *Can. J. Biochem. Physiol.* **37,** 911–917
18. Andrade, M. A., Chacón, P., Merelo, J. J., and Morán, F. (1993) Evaluation of secondary structure of proteins from UV circular dichroism spectra using an unsupervised learning neural network. *Protein Eng.* **6,** 383–390
19. Hunke, C., Chen, W. J., Schäfer, H. J., and Grüber, G. (2007) Cloning, purification, and nucleotide-binding traits of the catalytic subunit A of the V1VO ATPase from *Aedes albopictus*. *Protein Expr. Purif.* **53,** 378–383
20. Wimmer, R., Andersen, K. K., Vad, B., Davidsen, M., Mølgaard, S., Nesgaard, L. W., Kristensen, H. H., and Otzen, D. E. (2006) Versatile interactions of the antimicrobial peptide novispirin with detergents and lipids. *Biochemistry* **45,** 481–497
21. van Meer, G., Voelker, D. R., and Feigenson, G. W. (2008) Membrane lipids: where they are and how they behave. *Nat. Rev. Mol. Cell. Biol.* **9,** 112–124
22. Davison, S. C., and Wills, E. D. (1974) Studies on the lipid composition of the rat liver endoplasmic reticulum after induction with phenobarbitone and 20-methylcholanthrene. *Biochem. J.* **140,** 461–468
23. Li, H., Robertson, A. D., and Jensen, J. H. (2005) Very fast empirical prediction and rationalization of protein pK_a values. *Proteins* **61,** 704–721
24. Dolinsky, T. J., Nielsen, J. E., McCammon, J. A., and Baker, N. A. (2004) PDB2PQR: an automated pipeline for the setup of Poisson-Boltzmann electrostatics calculations. *Nucleic Acids Res.* **32,** W665–667
25. Kampmann, T., Mueller, D. S., Mark, A. E., Young, P. R., and Kobe, B. (2006) The role of histidine residues in low-pH-mediated viral membrane fusion. *Structure* **14,** 1481–1487
26. Rötzschke, O., Lau, J. M., Hofstätter, M., Falk, K., and Strominger, J. L. (2002) A pH-sensitive histidine residue as control element for ligand release from HLA-DR molecules. *Proc. Natl. Acad. Sci. U.S.A.* **99,** 16946–16950

Protein Structure and Folding:

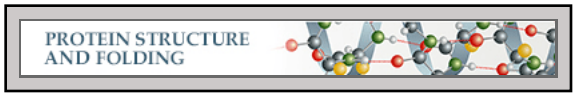

The Stem Region of Premembrane Protein Plays an Important Role in the Virus Surface Protein Rearrangement during Dengue Maturation

Qian Zhang, Cornelia Hunke, Yin Hoe Yau, Vernon Seow, Sumarlin Lee, Lukas Bahati Tanner, Xue Li Guan, Markus R. Wenk, Guntur Fibriansah, Pau Ling Chew, Petra Kukkaro, Goran Biukovic, Pei-Yong Shi, Susana Geifman Shochat, Gerhard Grüber and Shee-Mei Lok

J. Biol. Chem. 2012, 287:40525-40534.
doi: 10.1074/jbc.M112.384446 originally published online October 3, 2012
